Ocean Engineering 141 (2017) 108–115

Contents lists available at ScienceDirect

Ocean Engineering

journal homepage: www.elsevier.com/locate/oceaneng

The application of Froude scaling to model tests of Oscillating Wave Surge Converters

Pál Schmitt*, Björn Elsäßer

Marine Research Group, Queen's University Belfast, Northern Ireland, United Kingdom

ARTICLE INFO

Keywords:
OWSC
CFD
OpenFOAM
Froude scaling
Wall functions
Experimental tank test

ABSTRACT

Experimental tank testing of scale models is a standard tool in marine engineering. The underlying problem is well understood and refinements to standard applications, like resistance testing of typical ship hulls, have led to widely accepted methodologies. Similarly Reynolds-averaged Navier-Stokes computational fluid dynamics solvers have been used to assess the effect of scaling from model to full scale for ships successfully. Problems still arise when new structures, with very different shapes or modes of motion, are tested. The OWSC is such a new structure, and this paper investigates whether Froude scaling is adequate to extrapolate model scale tank testing to full scale devices. Since only limited full scale data is yet available, the investigation is mainly based on numerical simulations. It is shown that for current designs Froude scaling of typical tank scales is probably appropriate. The application of Reynolds-averaged Navier-Stokes computational fluid dynamics methods to scaling issues in the wave energy industry is demonstrated and some challenges, mainly the demands of industry standard wall functions on appropriate mesh resolution highlighted. Although the observed changes in flow patterns seem reasonable and can be explained by changes in viscosity, some uncertainty remains on the influence of mesh resolution.

1. Introduction

The Oscillating Wave Surge Converter (OWSC) consists of a buoyant, bottom hinged flap. It penetrates the water column completely and rotates back and forth around the hinge when acted upon by waves. This motion is used to drive a power take off system and generate electricity (Whittaker et al., 2007). The second prototype, build by the company Aquamarine Power Ltd. was tested at the European Marine Energy Center. It is 26 m wide and about 15 m high.

Most tank testing in the area of marine engineering, and thus most numerical and experimental methods, are developed for propulsion, resistance or manoeuvring of ships. The objective of ship or propeller design is to find an optimal shape with little resistance. Almost all shapes encountered in technical fluid dynamics, from wings, fans, propellers, turbines, ducts, cars, ships or submarines are streamlined.

While heaving buoys might be fairly similar to ships, an oscillating bottom hinged flap in a free surface flow is different from any other known technical off-shore structure. Firstly, the dominant fluid motion in the boundary layer is perpendicular to the flap's face and direction of motion. Secondly, the flap is an extremely blunt body and large areas of flow separation can be observed in the tank. These separation areas are not simply moved away by the waves, as they might be in typical hull resistance testing, but are constantly moved back and forth around the flap.

Depending on wave and flap characteristics the model or full scale flap might operate anywhere in a fully turbulent or even creeping flow. Changes can even be expected over the height of the flap. Short or small amplitude waves will not induce velocities close to the bottom, while in extreme waves, at very large rotation angles and high flow velocities, the flap seems similar to a flat plate and will experience significant viscous force components (Henry et al., 2014). The shape of OWSCs might vary considerably as shown in the study by Schmitt et al. (2013), further complicating general conclusions.

The boundary layer development is expected to affect the separation at the sides and maybe the flow close to the bottom. The influence of the bottom boundary layer is limited to the area close to the bottom and close to the hinge. Scaling errors in the velocities of the incoming flow field around the hinge will contribute little to the pitching moment. For sediment transport this might be of concern but for power output estimations they seem of little importance. Depending on the shape of the side effector, the location of the separation point is expected to vary for different scales. A sharp edge will force separation at small and large velocities alike. Rounded shapes will behave similar to the sphere in Prandtl's famous experiment (Prandtl, 1965) and are

* Corresponding author.
E-mail address: p.schmitt@qub.ac.uk (P. Schmitt).

http://dx.doi.org/10.1016/j.oceaneng.2017.06.003
Received 22 October 2015; Received in revised form 2 December 2016; Accepted 3 June 2017

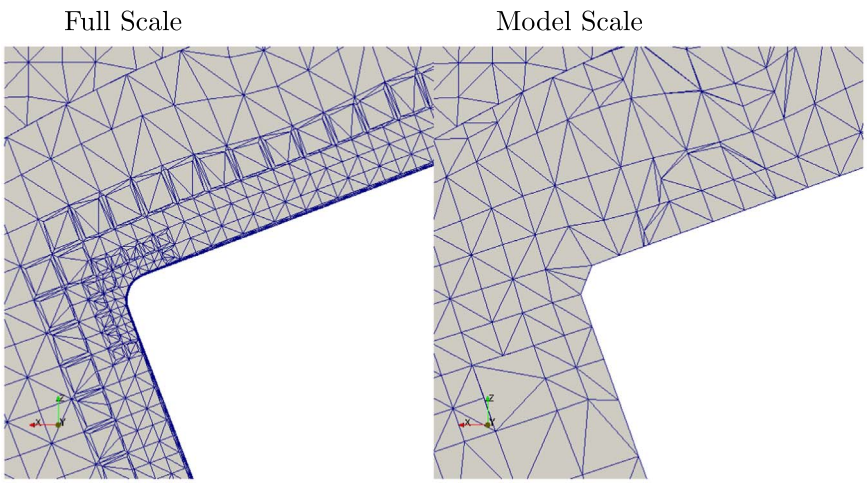

Fig. 1. Mesh refinement around flap. Boundary layer refinement for low viscosity (left) and standard case (right).

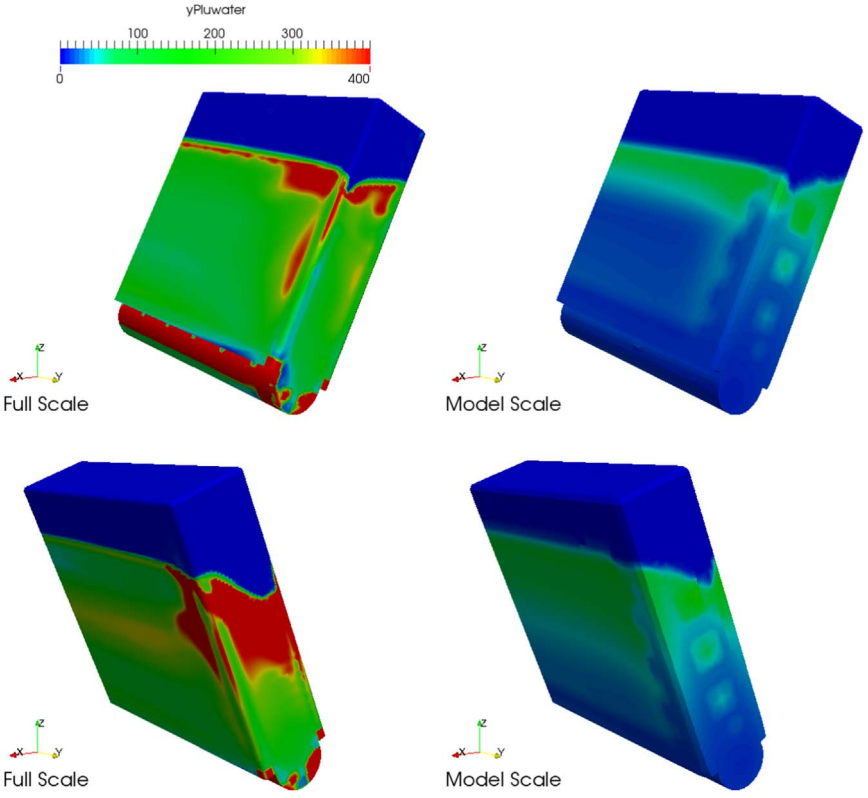

Fig. 2. Wall distance y^+ for model scale and equivalent full-scale simulation for different time steps in a wave cycle. (For interpretation of the references to color in this figure legend, the reader is referred to the web version of this article.)

thus difficult to predict and more likely to be wrongly simulated in the tank. At the same time, the effect of the form of the side on performance is not well understood.

Since the mode of operation of WECs varies considerably across the industry, and because of the issues discussed above, it is not possible to define a suitable Reynolds number for reliable tests. Recommended scales are 1:40 or above, although for floating, ship-like structures, scales of 1:100 might still be suitable (Holmes and Nielsen, 2010).

The physical background of scaling issues, that is the deviation in Reynolds number when the Froude number is conserved and vice versa, has been discussed in great detail for the case of wave power converters in general (Sheng et al., 2014) and are also commonly referred to in industry guidelines (Holmes and Nielsen, 2010). In general, Froude scaling is the only possible option when testing prototypes of wave energy converters, since water is the only medium available in test tanks. Researchers agree that above a certain Reynolds number, the flow regime is fully turbulent and coefficients of drag tend to become almost constant for a high Reynolds number range.

In many technical applications like pipes or propellers the choice of characteristic length and velocity has been standardised and thus Reynolds number dependent force coefficients are readily available. In other cases, for example WECs, defining a suitable Reynolds number is not trivial. The characteristic length scale of a device might not be readily defined or even vary depending on the aim of the investigation. For OWSCs the width of the flap could be used, based on the assumption that the most similar case is a thin plate perpendicular to the flow direction. If the flow between the bottom of the flap and the sea floor was of interest, it would of course be better to obtain similar

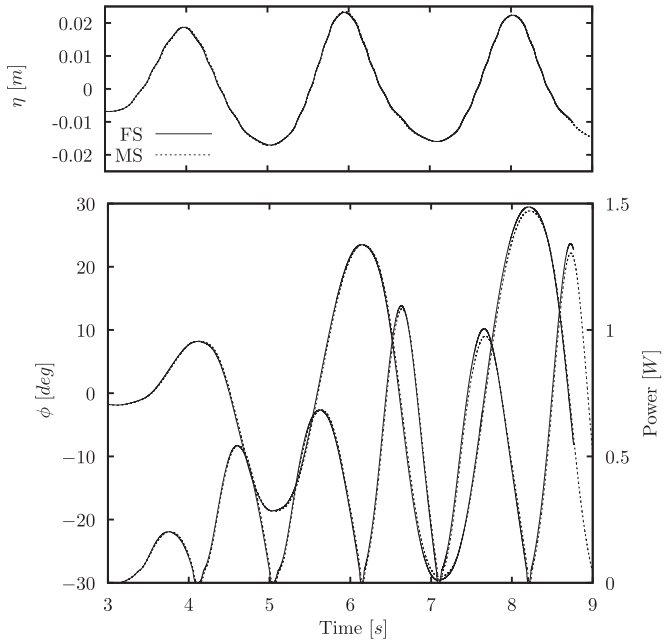

Fig. 3. Numerical results for surface elevation (top) and rotation angle (bottom) over time for full scale and model scale viscosity ratio.

Reynolds numbers for the height of the gap. Similarly one could argue the thickness of the flap is the characteristic length if vortex shedding around the sides is of interest. In the end, the Reynolds number is just a measure to assess the change in ratio of viscous to gravity forces when scaling is applied.

Drag coefficients of objects similar to OWSCs, though in single phase, unidirectional flow have been presented by Hoerner (1965). He discusses the drag of plates normal to the flow. At a sufficiently sharp corner, any boundary layer, turbulent or laminar, will separate. The drag coefficient of a plate above a Reynolds number (using the width as characteristic length) of about 400 is constant. For lower Reynolds numbers a peak in drag forces can be observed for a Reynolds number of about 300 which is reported to be due to a change in vortex shedding regime. Below a Reynolds number of about 100 a steep increase in drag can be observed. Munson et al. (2005) presented similar variations of drag for different shapes. The perpendicular plate shows no variation of drag over the whole range of Reynolds numbers from $10^4 - 10^7$. This is due to the fact, that the sharp edges force separation of the flow at low Reynolds numbers at a defined position. On other shapes the separation point changes with Reynolds number. The biggest variation in drag occurs for a flat plate aligned with the flow that experiences almost pure viscous forces which change considerably for different Reynolds numbers. Schmitt et al. (2012) presented viscous simulations of waves acting on a fixed flap, and already found that the viscous component was less than 1% of the pressure force, indicating that scaling might not be a major issue for typical tank tests.

A detailed discussion of the suitability of Reynolds and also the Keulegan-Carpenter numbers to choose appropriate sizes for scale testing of an OWSC is given by Clabby (2013).

Only one comparison between full scale field data and 40^{th} scale tank tests is available to date (O'Boyle et al., 2015). Error estimates of about +4% and −6% in power production probably mask the effect of variations in viscosity.

Recently simulation tools modelling viscous effects like Reynolds-averaged Navier-Stokes (RANS) equation solvers have been shown to be able to reproduce experimental tank tests with very high accuracy (Schmitt and Elsässer, 2015). Additionally they provide access to viscous and pressure force components, allowing to improve assessments of scaling errors. At the same time, the modelling employed in those tools, especially in the treatment of the near wall boundary layers, is sometimes ignored or not employed correctly, leading to the wrong assumption that if RANS tools can recreate tank effects, scaling effects can easily be assessed by simulating a full scale case. This paper presents a careful numerical simulation of an OWSC at different scales, highlighting possible sources of errors and limitations of those methods.

Tank tests have provided important results for the functioning of the bottom hinged flap. Since it is not possible to differentiate between viscous and pressure forces or to visualize the flow velocities close to the flap, variations in the flow regime for different shapes and wave characteristics can hardly be identified and quantified.

To assess the error introduced by applying Froude scaling to model scale results the following questions need to be answered:

1. Is the viscous force component relevant?
2. Does flow separation occur and if yes, does it change and thus influence the pressure force significantly?

2. Numerical investigation

Numerical methods solving the Navier Stokes Equations could in theory easily provide answers to these questions, but to achieve results with reasonable numerical effort some simplifications have to be introduced to the equations.

In most marine engineering applications RANS equations are employed. The velocity is split into a time-averaged $\overline{u}$ and fluctuating component u'. Replacing the velocity u with $\overline{u} + u'$ yields the Navier Stokes equations for $\overline{u}$. The fluctuating components cancel out except for one additional term, which can be interpreted as an additional viscosity term μ_t, so that the equations for u and $\overline{u}$ are almost identical. Additional equations are then required to solve for μ_t and are usually based on coupling the production and dissipation of turbulent kinetic energy with the mean velocity.

The equations for the turbulence properties of the RANS equations introduce new properties and no closed solution has yet been found. The closure problem is overcome by applying some empirical knowledge and boundary conditions for the variables describing the turbulence. For example the most common RANS models are the $k - \epsilon$ and $k - \omega$ model. k is a variable describing the turbulent kinetic energy, ϵ or ω are dissipation or frequency related terms. The turbulence model consists of transport equations and describe the transport, production and dissipation of these properties.

Special care is required to set the boundary conditions at walls or inflows for these properties. In the simulations presented later, the are no inflow boundaries and the computations begin from still water, so consequently turbulence is created during run-up and close to zero turbulence was used as initial condition.

Some models can be used up to the wall and a standard boundary condition like zero gradient can be used. In practice, this is often not feasible due to the required computational effort, and thus often the boundary layer is modelled without resolving the very thin viscous sub layer, using so called wall functions (Ferziger and Peric, 2002). These wall functions are based on the universal law of the wall, which was first described by Theodore von Kármán. It should be noted however, that the law of the wall is only a non-dimensional description which fits many observed turbulent boundary layers, but not an actual law of physics. It typically holds true for flows along a boundary, but of course breaks down during flow separation or in regions of reversing flows. With the shear stress on the wall τ_W the shear velocity can be calculated as

$$u_\tau = \sqrt{\frac{\tau_W}{\rho}} \tag{1}$$

The non dimensional wall distance Y^+ is defined as

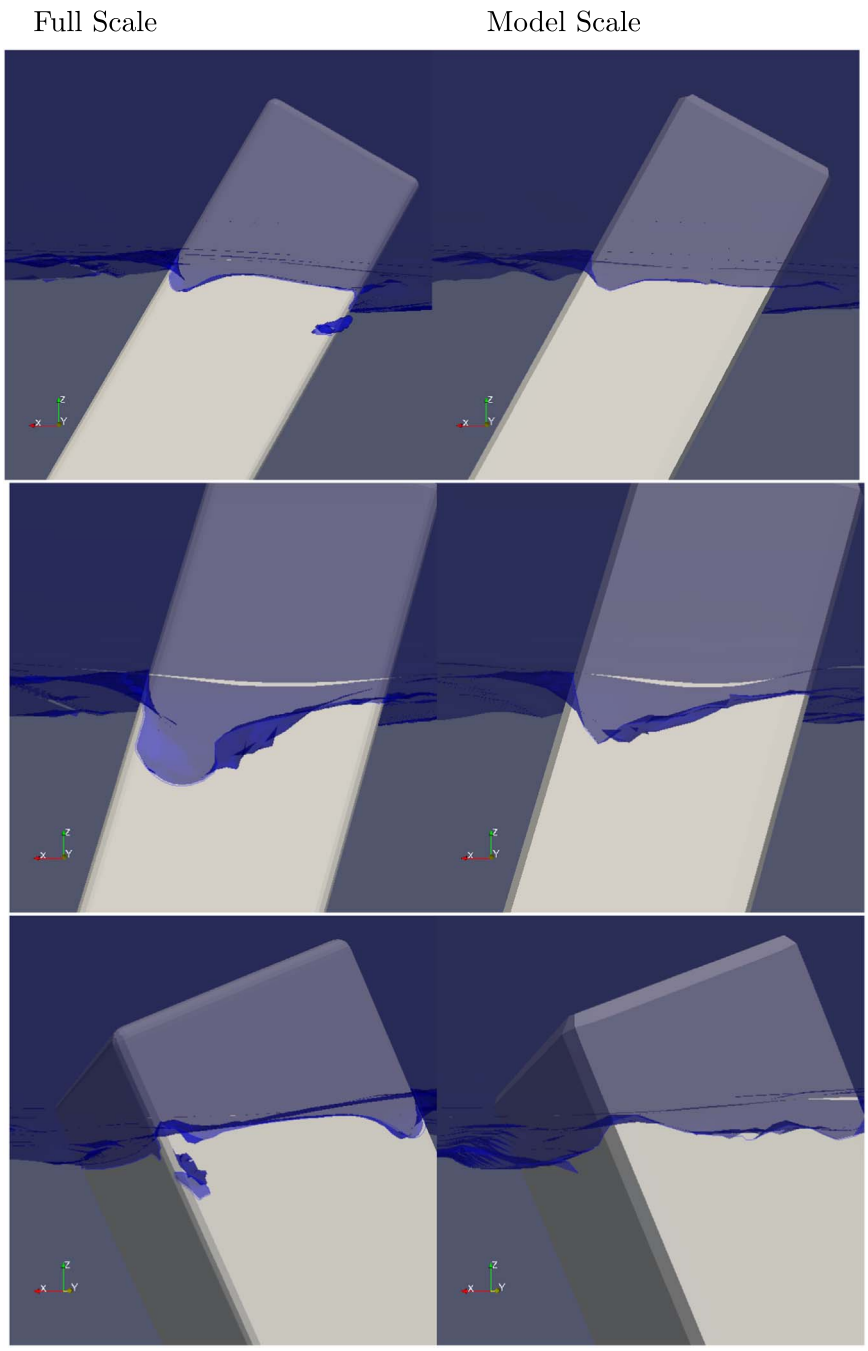

Fig. 4. Surface elevation at the side of the flap for model scale and equivalent full-scale simulation for different time steps.

$$Y^+ = \frac{yu_\tau}{\nu} \tag{2}$$

The non dimensional velocity $u^+ = \frac{u}{u_\tau}$ is then described between $Y^+ = 20$ and $Y^+ = 350$ by

$$u^+ = \frac{1}{\kappa} lnY^+ + C^+ \tag{3}$$

This region is thus called the logarithmic or log-law region.

More advanced schemes exist, that switch between different functions, depending on the value for Y^+. For example the viscous sub-layer for $Y^+ < 5$ can be described by

$$u^+ = Y^+ \tag{4}$$

Wall functions using only the logarithmic relations are also called high Reynolds number wall functions and require the center of the cell closest to a wall boundary to be within the valid range of Y^+. Creating a suitable mesh can be challenging, especially if the local velocities are unknown beforehand. Y^+ can and should be evaluated in the post-processing to control the validity of the underlying assumptions. In this study the standard kOmegaSST turbulence model was used.

Recently Wei et al. (2015) presented a numerical study of OWSCs using RANS CFD methods and concluded that Froude scaling was appropriate down to 100th scale. The same mesh was used in all simulations and although different RANS turbulence models were tested and shown to give identical results there is no information on the wall functions used or on the resolution of the boundary layer.

The case presented here is based on the work described in detail in Schmitt and Elsässer (2015). The computational domain is 21.3 m long, 2.58 m wide and 1.17 m high. The water level is 0.691 m and the wavemaker is set to produce a wave with a period of 2.055 s and a wave

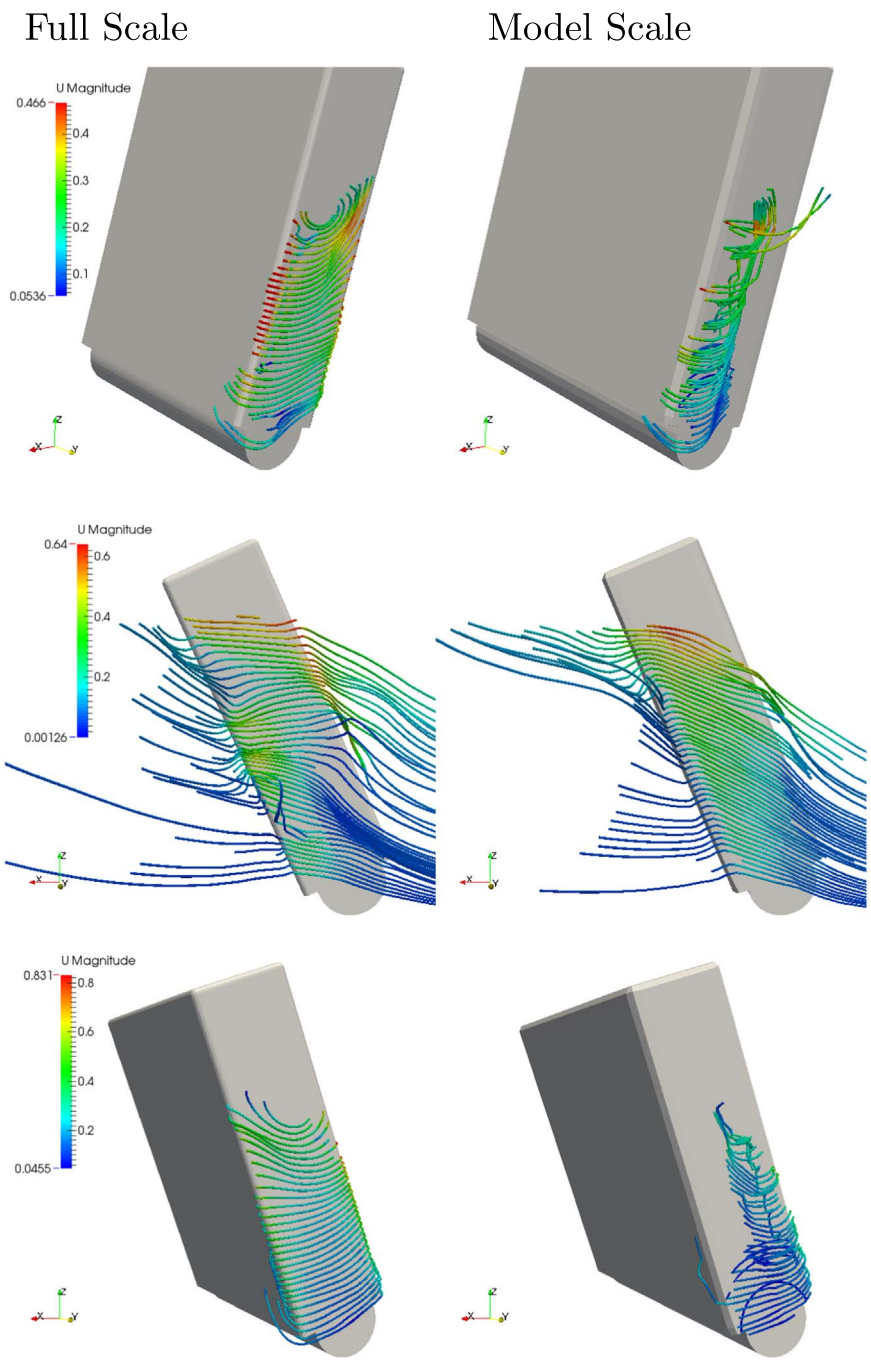

Fig. 5. Streamlines around the side of the flap for model scale and equivalent full-scale simulation for different time steps.

height of about 0.04 m. The solver is based on the interFoam Volume of Fluid solver provided by OpenFOAM. A numerical beach minimizes reflection at both ends of the tank.

Instead of scaling the flap model and tank, a numerical model allows changes to the viscosity of the fluids to obtain Reynolds similitude. This set-up resembles small scale testing at correct Froude numbers and simplifies post-processing since the plots are created identically. Although the size of the domain is unchanged, results for the correctly scaled case are named full scale (*FS*) in the remainder of this document.

The relationship for the correct Froude scaling of viscosity is derived from the basic relations of distance and time as follows

$$\nu_{Modell}\,[m^2/s] = \frac{\lambda^2}{\sqrt{\lambda}}\nu = \lambda^{3/2}\nu \tag{5}$$

The values for viscosity used in *MS* and *FS* simulations at 40*th* scale are

	MS	*FS*	
ν_{Water}	$1E-6$	$3.95E-09$	[m²/s]
ν_{Air}	$5.85E-8$	$2.3E-10$	[m²/s]

The mesh has to be adapted to account for the much smaller boundary layer at full scale, see Fig. 1.

Fig. 2 shows the non dimensional wall distance Y^+ under the water surface on the flap for both cases for two different time steps, close to the extreme rotation amplitudes. The color scale has been adjusted to show values where the log-law of the wall function is valid in green. Too small values are shown in blue, too large ones in yellow to red. It can be observed that in different areas on the flap the wall distance becomes too large or too small over the wave cycle. The model scale case is only

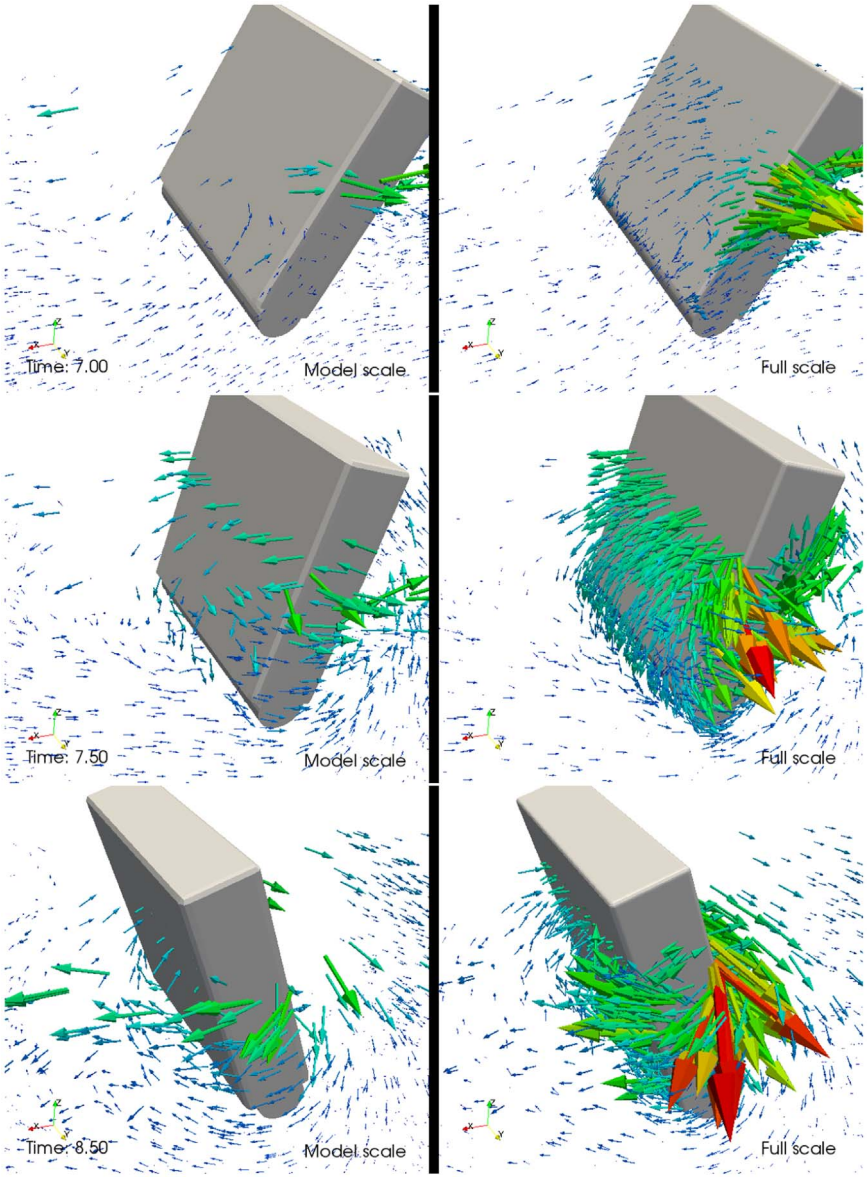

Fig. 6. Flow field around the flap for model scale and equivalent full-scale simulation for different time steps.

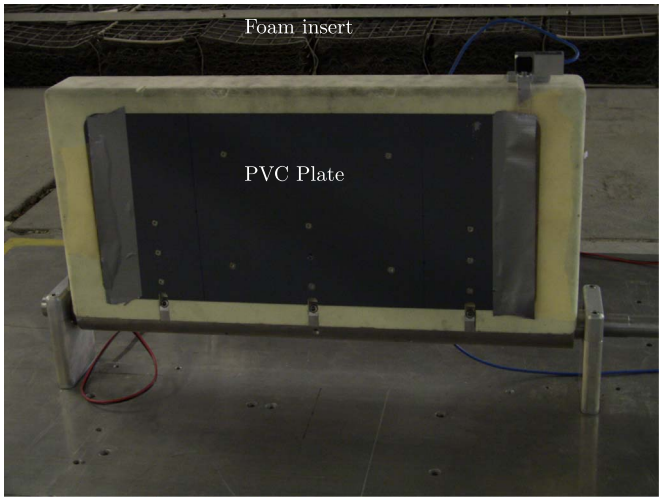

Fig. 7. Photograph of flap and support structure.

well resolved on the upper third of the flap, the full scale case is well resolved on the flap faces but the mesh is still too coarse on the sides and around the hinge.

More refined boundary meshes increase the run time considerably. While in 24 h 15 s of time were simulated for the model scale, less than 9 s of simulation time of the full scale case took 72 h on 32 cores of run time to complete. The mesh size increases from 1,007,518 cells for the model scale case by about 30% to 1,333,930 cells for full scale. Since the differences in results are already minimal, both cases were re-run with the same maximum time-step of 1E-04s. That timestep was found by first running the full scale case with an adaptive time step, limited by a Courant number of 0.5.

An analysis of the force components shows that, as expected in previous considerations, the viscous shear force component in wave propagation direction is less than 0.1% of the total force for any point in time. Scaling errors due to variations in shear stress or inaccuracies in the simulation of shear forces in CFD simulations are thus negligible.

Fig. 3 shows the surface elevation and the rotation angle for both cases. Viscosity is not expected to play any significant role in wave propagation and no difference can be observed between the surface elevation for both cases.

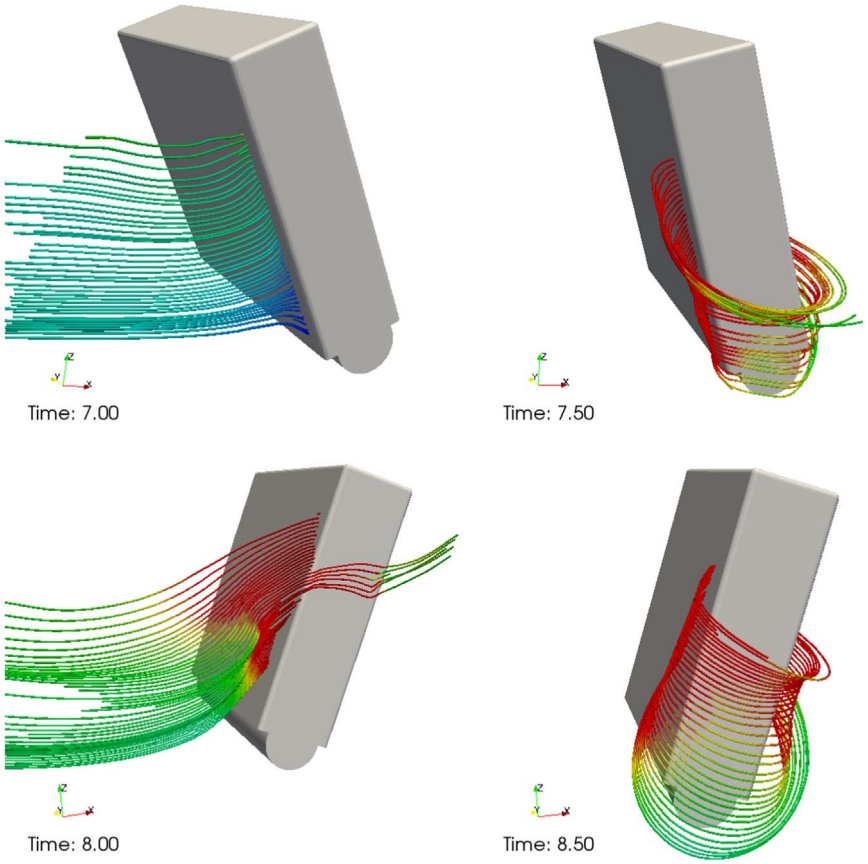

Fig. 8. Streamlines originating from mesh position for different time steps.

The flap in the full scale case begins to rotate with increasingly larger amplitudes compared to the model scale. The available data does not show whether the flap rotation has settled yet, after 8.5 s the full scale flap reaches about 2% larger rotation angles than the model scale. Power output is also 3% larger for the full scale case. These minor differences, though plausible to be caused by variations in viscosity, could also stem from changes in mesh resolution. Since the mesh resolution is defined by the wall distance it is impossible to perform a mesh convergence study.

Fig. 4 shows the surface beside the flap for both scales at different time-steps. A bubble can be observed in the water for the full scale case while the surface deformation seems very similar for both cases. Half a second later the flaps are almost upright and a drop in the surface beside the flap can be observed for both cases. This trough is about twice as deep than for model scale and much wider, forming a round shape. After a further 0.5 s, with the flaps leaning against the incoming wave direction, another bubble can be observed separating from the front edge for the full scale case. The full scale case also shows a relatively sharp rise in surface elevation at the front edge and a drop at the back edge, forming two distinct dents in the surface. Around the model scale case the surface seems a lot smoother, no bubbles or sharp deformations can be observed. Obviously the coarser mesh for the tank scale could not possibly resolve a small bubble close to the body and the differences seen might be due to the different mesh resolution. Surface tension is also not considered in the solver and the water surface is merely reconstructed from the flow field, so these results should be treated with care. It should be noted though, that splashes and bubbles are visible around the full scale device in operation (see: https://youtu.be/S4O0JcNfTKo) while during 40*th* and 25*th* scale tank tests in equivalent wave conditions no splashing is observed.

Fig. 5 shows visualizations of the flow around the edge. Streamlines were calculated 0.33 m from the center of the tank, just beside the flap.

At the first time-step the flow can be seen to pass smoothly beside the flap for the full scale case, while the model scale case shows the formation of a vortex, spanning from the hinge and opening wider towards the surface.

Half a second later the flow seems slightly more turbulent around the full scale case, the streamlines at model scale are almost parallel to each other.

Another half a second later a vortex can be observed again beside the flap in the model scale case, but not for the full scale simulation.

More significant differences in the flow field can be observed in a three dimensional flow analysis around the flap, Fig. 6. For all time-steps the velocities of the flow around the side is higher for the full scale flap. Although some high velocity is induced by the air bubbles in the flow, the difference is significant and can be observed over the entire height of the flap. It can also be observed how the water is squeezed sideways, creating transverse flows towards the sides on one flap face and similar flow patterns in opposite direction on the other.

Viscous shear is created by highly rotational flows and creates resistance. Forcing the water to flow around the side (and hinge) will cost relatively more energy and increase resistance of the flap if viscosity is higher, even if the shear force is not directed in the direction of motion of the flap.

3. Experimental investigation

Experiments were performed at the wave tank in Queen's University Belfast to investigate if forcing a transition of the boundary layer to turbulent flow would change it's behaviour. The experimental set-up is almost identical to the one described in detail in Schmitt and Elsässer (2015).

The wave tank at Queen's University's hydraulic laboratory is 4.58 m wide and 20 m long. An Edinburgh Design Ltd. wave-maker

with 6 paddles is installed at one end. The bottom is made of concrete slabs and sloped, two horizontal sections allow experimental testing 150 mm and 356 mm above the lowest floor level at the wave-maker. A beach consisting of wire meshes is located at the opposite end.

The flap model consists of three units, the fixed support structure, the hinge and the flap.

The flap itself is made of a foam center piece, sandwiched by two PVC plates on the front and back face, Fig. 7.

Pieces of mesh were fixed onto the faces of the flap, just behind the side edges to force transition to turbulent flow. The mesh is not lying flat on the flap face but stands out a few millimetres. Since the width of the flap and thus the area on which the dominating pressure force acts remains equal, any difference in flap rotation could be attributed to some change in flow regime around the sides. To keep changes to the set-up to a minimum, experiments were prepared with the mesh, during test runs the mesh was removed without draining the tank or doing any changes to the rest of the set-up.

Experiments performed in monochromatic waves showed no measurable difference for test runs with and without the attached mesh. Simulation results indicate that little flow from the mesh position goes directly around the sides, Fig. 8. While this could explain why the mesh has no measurable effect on rotation in the experiments it rather seems to be another confirmation of earlier conclusions that the OWSC is not likely to be severely affected by scale effects.

4. Conclusions

Simulations varying the viscosity of the fluids to obtain Froude and Reynolds similitude show up to 2% larger rotation angles and 3% higher power output when compared to model scale simulations. Significant differences in the surface deformation and the flow around the sides can be observed. Although these results are to be expected, at least qualitatively, from fundamental fluid dynamics, some effects might be due to variation in mesh resolution. Due to the use of wall functions, which define the necessary wall distance, no mesh refinement study can be performed, highlighting some deficiencies of these numerical tools. RANS Simulations resolving the boundary layer in more detail or even LES methods could improve the understanding and confidence in these results but also increase the computational effort by orders of magnitude. Considering the high computational cost, even if wall functions are employed, smaller scale simulations seem to be impractical due to constraints in meshing and computational effort. With regards to the difficulties encountered when complying with the requirements of typical wall functions, it is unclear how (Wei et al., 2015) obtained correct results at 100^{th} scale without localised mesh variation.

Full scale simulations show the separation of bubbles close to the edges. Model scale simulations show the formation of a vortex beside the flap, while the water passes unhindered at full scale. Although problems persist in meshing to resolve the wall distance correctly and wall functions may well fail in oscillating flows, results seem to indicate that in small scale model tests the formation of a vortex besides the flap creates some additional drag, reducing the rotation amplitude.

Viscosity will also play an important role in the transverse flows observed on the flap faces and thus lower viscosity will decrease the resistance of the flap.

Observed differences seem to stem from flow effects related to the side edges. The significance of the error introduced by applying Froude scaling to experimental model scale tests will depend (besides the scale and wave conditions) on the flap geometry and shape of the sides. Especially scale models with a small gap below the flap will underestimate the flow and associated losses in driving forces.

Experimental tests, attempting to force transition of the boundary layer to turbulence, also showed no influence on rotation.

Acknowledgements

Pál Schmitt's Ph.D. was made possible by an EPSRC Industrial Case Studentship 2008/09 Voucher 08002614 with industrial sponsorship from Aquamarine Power Ltd. Their support is much appreciated.

References

Clabby, D., 2013. Comparison of the Performance of a Full Scale Wave Energy Converter to that of its Physical Model. (Ph.D. thesis). The Queens University of Belfast.

Ferziger, J., Peric, M., 2002. Computational Methods for Fluid Dynamics 3 ed.. Springer, Berlin, Heidelberg.

Henry, A., Rafiee, A., Schmitt, P., Dias, F., Whittaker, T., 2014. The characteristic of wave impacts on a oscillating wave surge converter. J. Ocean Wind Energy, 101–110.

Hoerner, S.F., 1965. Fluid-dynamic drag: practical information on aerodynamic drag and hydrodynamic resistance. Hoerner Fluid Dynamics, Vancouver, Alburqueque, N.M.

Holmes, B., Nielsen, K., 2010. Guidelines for the Development and Testing of Wave Energy Systems. Technical Report. OES IA Document No: T02-2.1.

Munson, B., Young, D., Oshiki, T., 2005. Fundamentals of Fluid Mechanics. John Viley & Sons, New York.

O'Boyle, L., Doherty, K., van't Hoff, J., Skelton, J., 2015. The value of full scale prototype data - testing Oyster 800 at EMEC, Orkney. In: Proceedings of the 11th European Wave and Tidal Energy Conference.

Prandtl, L., 1965. Fuehrer durch die Stroemungslehre. Vieweg, Braunschweig/Wiesbaden.

Schmitt, P., Elsässer, B., 2015. On the use of OpenFOAM to model oscillating wave surge converters. Ocean Eng. 108, 98–104. http://dx.doi.org/10.1016/j.oceaneng.2015.07.055, (URL ⟨http://www.sciencedirect.com/science/article/pii/S0029801815003686⟩).

Schmitt, P., Bourdier, S., Sarkar, D., Renzi, E., Dias, F., Doherty, K., Whittaker, T., van't Hoff, J., 2012. Hydrodynamic loading on a bottom hinged oscillating wave surge converter. In: Proceedings of the Twenty-second (2012) International Offshore and Polar Engineering Conference, International Society of Offshore and Polar Engineers (ISOPE), pp. 550–557.

Schmitt, P., Doherty, K., Whittaker, T., 2013. Shape optimization of a bottom hinged flap type wave energy converter. In: Grabe, J. (Ed.), Conference on Maritime Energy, pp. 47–61.

Sheng, W., Alcorn, R., Lewis, T., 2014. Physical modelling of wave energy converters. Ocean Eng. 84, 29–36. http://dx.doi.org/10.1016/j.oceaneng.2014.03.019, (URL ⟨http://www.sciencedirect.com/science/article/pii/S0029801814001085⟩).

Wei, Y., Rafiee, A., Henry, A., Dias, F., 2015. Wave interaction with an oscillating wave surge converter, Part I: viscous effects. Ocean Eng. 104, 185–203. http://dx.doi.org/10.1016/j.oceaneng.2015.05.002, (URL ⟨http://www.scopus.com/inward/record.url?eid=2-s2.0-84936880408 & partnerID=40 & md5=e2c579932d459660fbfbc591ce5a7b14⟩) cited By 0..

Whittaker, T., Collier, D., Folley, M., 2007. The development of Oyster - a shallow water surging wave energy converter, In: Proceedings of the 7th European Wave and Tidal Energy Conference.